

Bandgap Wavelength Shift in Quantum Well Intermixing using Different SiO₂ masks for Photonic Integration

Jieun Lee¹, Yoshiaki Yamahara¹, Mitsuaki Futami¹, Takahiko Shindo²,
Tomohiro Amemiya², Nobuhiko Nishiyama¹, and Shigehisa Arai^{1,2}

¹Department of Electrical and Electronic Engineering, ²Quantum Nanoelectronics Research Center
Tokyo Institute of Technology, Meguro-ku, Tokyo 152-8552, Japan

Email address: lee.j.aj@m.titech.ac.jp

Abstract—As a photonic integration method of semiconductor membrane structure, quantum-well-intermixing (QWI) process using O₂-sputtered SiO₂ mask was investigated by comparing the photoluminescence peak wavelength shift between two sections with/without the SiO₂ mask. As the result, a large bandgap wavelength difference of 80 nm (47 meV) was obtained while quite large transient region (90 μm) was observed. Since this fact was considered to be attributed to the temperature gradient along the masked and window regions during the rapid thermal annealing (RTA) process, we deposited CVD SiO₂ (which has smaller vacancies than O₂-sputtered SiO₂ hence the bandgap wavelength shift is smaller) on the entire surface after forming O₂-sputtered SiO₂ mask pattern and successfully reduced the transient region length to less than 5 μm.

Keywords—quantum-well intermixing (QWI); photonic integration; membrane photonic integrated circuits

I. INTRODUCTION

To realize the optical interconnections on a Si-LSI, we proposed the concept of the membrane photonic integrated circuit (PIC) [1] as shown Fig. 1, and reported its components such as a membrane laser [2], a photo-detector [3] and an InP-based waveguide [4]. As for the photonic integration method of active and passive devices, quantum-well-intermixing (QWI) is expected to be versatile technique by increasing in the bandgap wavelength and changing in the refractive-index partially, with only single epitaxial growth [5]. A great deal of intermixing techniques have been reported; impurity induced disordering (IID) [6], photoabsorption-induced disordering (PAID) [7], and impurity-free vacancy-enhanced disordering (IFVD) [8] in multiple applications. In this paper, we employ the IFVD mixing method, which relies on creating vacancies in the III-V semiconductor using SiO₂ mask during annealing process. In regard to the bandgap wavelength shift for formation of passive region, the SiO₂ mask margin and surface cover mask are considered as the key for wide bandgap wavelength shift value and sharp shift gradient on the boundary of active and passive regions.

II. QWI PROCESS

For the QWI process, the base structure shown in Fig. 2 (a) was grown on an n-InP wafer using organo-metallic vapor-phase epitaxy (OMVPE). The base structure consists of five 6-nm-thick quantum-wells and six 10-nm-thick barriers, sandwiched by 55-nm-thick 1.55Q (GaInAsP; λ_g = 1.55 μm) layers. Above the core layer, a 10-nm-thick InP was followed by 10-nm thick GaInAs cap layer designed to cover semiconductor surface during the heating process.

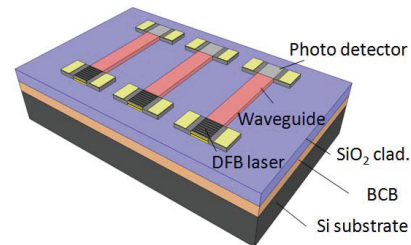


Fig. 1 Schematic representation of membrane photonic integrated circuits.

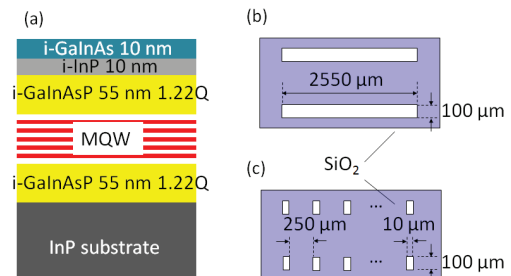
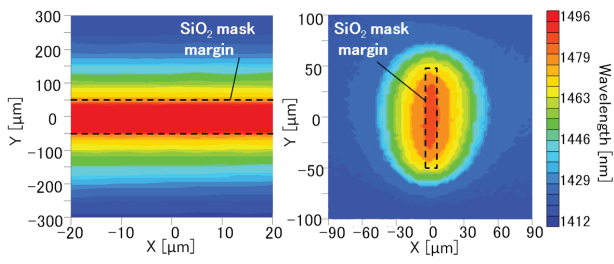


Fig. 2 (a) Epitaxial base structure with 5 quantum-well active region of 90 nm, (b) QWI-SiO₂ masks margin stripe type, and (c) island type.

The fabrication process is started with formation of photo-resist mask pattern of active region on the base structure by photolithography. Then, 200-nm-thick SiO₂ mask was deposited on the wafer by O₂-sputtering (5 sccm) with a pressure of 1.0×10⁻⁴ Torr at room temperature. Then the SiO₂ mask on the active region was removed by a lift-off process for remaining the mask margin and for QWI process. Finally, the rapid thermal anneal (RTA) was held at 750°C for 180 seconds in nitrogen atmosphere for creating vacancies in the III-V semiconductor. When the dielectric mask formed on III-V wafer was heated in the RTA process, Gallium atoms migrated into the SiO₂ mask layer created group III vacancies and inter-diffused through the quantum-well, then result in QWI.

III. QWI CHARACTERIZATION

In this study, 2 types of SiO₂ mask patterns were prepared; stripe pattern with 100×2550 μm² and island pattern with 100×10 μm² as shown in Figs. 2(b) and 2(c) to confirm the effect of mask margin to QWI. After the RTA was carried out, photoluminescence (PL) mapping with 3×3 μm² resolution was done. Figures 3(a) and 3(b) show the PL mapping results of stripe and island type patterns, respectively. In the stripe type, the bandgap wavelength shifts were 135 nm (76 meV) in the passive section (covered with SiO₂ mask) and 55 nm (29 meV) in the active section (without SiO₂ mask), hence the difference of 80 nm (47 meV) was obtained. The full width at half



(a) stripe type (b) island type
Fig. 3 PL mapping results of peak wavelength.

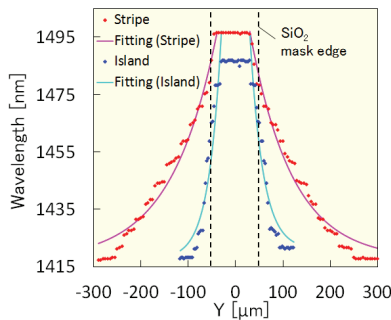
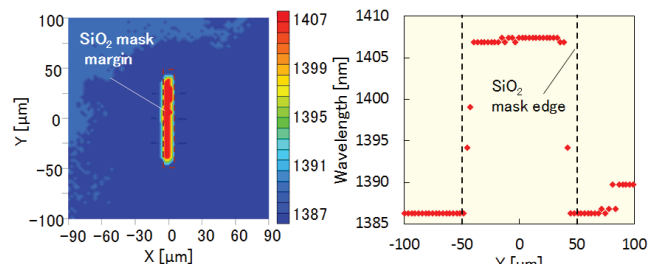


Fig. 4 Peak wavelength distribution depending on the distance from the mask center.

maximum (FWHM) was 41 meV in the passive section and was slightly wider than 35 meV in the active section. In the island type mask case, the shifts in the passive and the active sections were 130 nm (73 meV) and 60 nm (32 meV), respectively, and the difference was 70 nm (41 meV). The FWHM was 40 meV in the passive section and was 38 meV in the active section.

Although the wavelength shift difference between the two sections in the stripe pattern was wider than that in the island pattern, the transient region length was also wider. Figure 4 indicates the peak wavelength distribution depending on the distance from the center ($Y = 0$) of the mask. Since the PL peak wavelength shifted exponentially from the mask edge, we defined the transient region length as the distance where the PL wavelength shift becomes $1/e$ of the maximum wavelength shift such as diffusion constant. The transient region length was 90 μm for the stripe pattern and was 25 μm for the island pattern. From these results, we considered that this gradient was caused by the temperature gradient during the RTA process since the open window region is exposed to the ambient N_2 while the SiO_2 masked region is insulated.

In order to confirm the above mentioned assumption and to reduce the transient region length, a supplementary experiment was performed so as to decrease thermal conductivity difference between these two regions by covering the entire surface with additional SiO_2 film deposited by plasma enhanced chemical vapor deposition (PECVD) which has less defects than O_2 -sputtered SiO_2 . Figure 5(a) indicates the PL mapping result of peak wavelength, and Fig. 5(b) shows the peak wavelength distribution along the vertical direction. The transient region length was reduced to less than 5 μm . The bandgap wavelength shifts were 164 nm (95 meV) in the passive section and 143 nm (81 meV) in the active section, and the FWHMs were 47 meV (passive) and 49 meV (active). Even



(a) SiO_2 covered island type (b) PL distribution
Fig. 5 PL measurement results of peak wavelength in the SiO_2 covered island type.

though the wavelength shift difference was reduced to only 21 nm (14 meV) in this experiment, it is reasonable to assume that the wavelength shift total distance can decrease to 30 μm from 84 μm when the wavelength shift was supposed to 70 nm proportionally with same transient region as island pattern. Therefore, taking care of surface temperature distribution is very important to achieve sharp division for QWI.

IV. CONCLUSION

In conclusion, we investigated QWI process using SiO_2 mask for photonic integration and obtained the transient region length of less than 5 μm by combining 2 different SiO_2 masks to avoid the temperature gradient during the RTA process.

ACKNOWLEDGMENT

This work was supported by JSPS KAKENHI (Grant numbers 24246061, 24656046, 22360138, 21226010, 23760305, and 10J08973), the Council for Science and Technology Policy (CSTP) under the FIRST program, and the Ministry of Internal Affairs and Communications under the SCOPE program.

REFERENCES

- [1] S. Arai, N. Nishiyama, T. Maruyama, and T. Okumura, "GaInAsP/InP membrane lasers for optical interconnects," *IEEE J. Sel. Top. Quantum Electron.*, vol. 17, no. 5, pp. 1381-1389, Oct. 2011.
- [2] M. Futami et al., "Low-threshold operation of LCI-Membrane-DFB lasers with Be-doped GaInAs contact layer," *Proc. Int. Conf. Indium Phosphide and Related Materials*, Th-2C.5, Aug. 2012.
- [3] Y. Yamahara et al., "Characterization of GaInAsP lateral junction waveguide type membrane photodiode," the Institute of Electronics, Information and Communication Engineer, C-4-15, Sep. 2012.
- [4] J. Lee et al., "Low-loss GaInAsP wire waveguide on Si substrate with benzocyclobutene adhesive wafer bonding for membrane photonic circuits," *Jpn. J. Appl. Phys.* vol. 51, no. 4, pp. 042201-1-042201-5, Apr. 2012.
- [5] J. W. Raring et al., "Demonstration of widely tunable single-chip 10-Gb/s laser-modulators using multiple-bandgap InGaAsP quantum-well intermixing," *IEEE Photon. Technol. Lett.*, vol. 16, no. 7, pp. 1613-1615, July 2004.
- [6] D. Deppe and N. Holonyak, Jr., "Atom diffusion and impurity-induced layer disordering in quantum well III-V semiconductor heterostructures," *J. Appl. Phys.* vol. 64, no. 12, pp. 93-113, Dec. 1988.
- [7] B. Qui, A. Bryce, R. De La Rue, and J. Marsh, "Monolithic integration in InGaAs-InGaAsP multi-quantum-well structure using laser processing," *IEEE Photon. Technol. Lett.*, vol. 10, no. 6, pp. 769-771, June 1988.
- [8] S. K. Si, D.H. Yeo, K. H. Yoon, and S. J. Kim, "Area selectivity of InGaAsP-InP multi-quantum-well intermixing by impurity-free vacancy diffusion," *IEEE J. Sel. Topics Quantum Electron.*, vol. 4, no. 4, pp. 619-623, June/Aug. 1988.